

AD-A040 116

CARNEGIE-MELLON UNIV PITTSBURGH PA DEPT OF METALLURG--ETC F/G 11/3  
ALUMINIDE COATING ON DIRECTIONAL GAMMA'/DELTA EUTECTICS.(U)  
MAY 77 H C BHEDWAR, R W HECKEL, D E LAUGHLIN N00014-76-C-0198

UNCLASSIFIED

TR-1

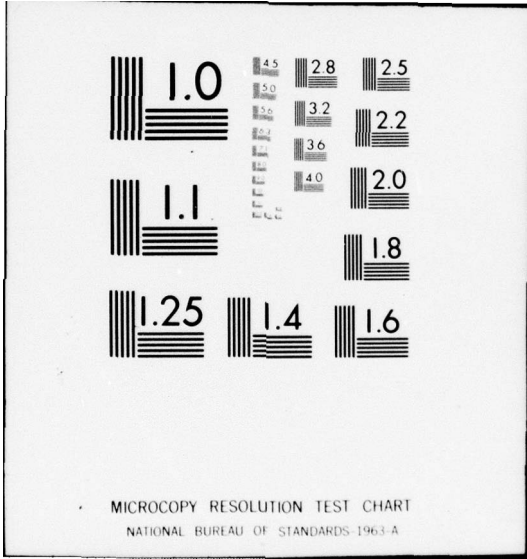
NL

1 of 1  
ADA040 116



END

DATE  
FILMED  
6-77



ADA 040 116

17

Z

Gamma/Delta

6 ALUMINIDE COATING ON DIRECTIONAL  $\gamma/\delta$  EUTECTICS.  
10 H. C. /Bhedwar, R. W. /Heckel, D. E. /Laughlin  
Homi Richard Avid

9 Technical Report, No. 1  
Office of Naval Research  
Contract N00014-76-C-0198  
11 May 1977

12 21p.

14 TR-1

15 N00014-76-C-0198

Reproduction in whole or in part is permitted for any purpose of the United States Government.

Distribution of this document is unlimited.

Carnegie-Mellon University  
Department of Metallurgy and Materials Science  
Pittsburgh, Pennsylvania 15213



DDC  
RECEIVED  
JUN 2 1977  
A

AD No. \_\_\_\_\_  
DDC FILE COPY

CDF 444 459

ALUMINIDE COATING ON DIRECTIONAL  $\gamma'/\delta$  EUTECTICS

H. C. Bhedwar, R. W. Heckel\* and D. E. Laughlin  
Department of Metallurgy and Materials Science  
Carnegie-Mellon University  
Pittsburgh, Pennsylvania 15213

APPROPRIATION FOR	
DIS	White Section <input checked="" type="checkbox"/>
DOC	Buff Section <input type="checkbox"/>
UNANNOUNCED	<input type="checkbox"/>
JUSTIFICATION.....	
BY.....	
DISTRIBUTION/AVAILABILITY CODES	
Dist.	AVAIL. AND/OR SPECIAL
	

ABSTRACT

The relationship between the process variables and the coating microstructure were studied for aluminide-coated  $\gamma'/\delta$  directional eutectics. A spectrum of coating microstructures were obtained depending on the choice of the process variables. The process variables were the aluminizing and homogenizing temperatures, the homogenizing time and the activity of aluminum in the coating pack. The microstructures were described with reference to the Ni-Al-Nb ternary phase diagram and the diffusion of the aluminum and the nickel atoms.

---

\*Now at Michigan Technological University, Department of Metallurgical Engineering, Houghton, Michigan 49931.

### INTRODUCTION

Recent studies on turbine blade materials have resulted in the development of in-situ composites. These materials possess an aligned second phase produced by the directional solidification of a eutectic. One system of interest is the directional  $\text{Ni}_3\text{Al-Ni}_3\text{Nb}$  ( $\gamma'/\delta$ ) eutectic.<sup>1</sup> Although the environmental behavior of such systems is important, only recently has the oxidation behavior of directional eutectics been studied.<sup>2,3</sup> These studies have recommended the use of oxidation-resistant coatings for long-term, high temperature service.<sup>1,2,4</sup>

Aluminide coatings on turbine blade materials have been used for a number of years as an efficient and low-cost protection system. While an extensive background on aluminide coatings exists in the literature,<sup>5,6,7,8,9,10</sup> the process variables/structure/property relationships are not adequately understood. A comprehensive study was therefore undertaken to examine the effects of the aluminide coating process variables on the oxidation behavior of  $\gamma'/\delta$  eutectics, through the control of the coating microstructure. In general, the coating microstructure can be altered by the following process variables: the aluminizing and homogenizing temperatures, the homogenizing time and the activity of aluminum in the coating pack. The homogenizing treatments were performed to determine the extent of coating degradation due to the high-temperature exposure of the coating, uncomplicated by the effects of oxidation. The ternary diffusion path<sup>11,12</sup> was used to monitor the changes in the coating microstructure since each of the above process variables affects one of the terminal compositions (the surface composition) of the coated

substrates.

This paper presents the results of a shorter study on the effects of the aluminide coating process variables on the microstructure of the coated substrates. It deals with the mechanisms of coating formation (aluminization) and degradation in an inert environment (homogenization). The sequence of the phase layers in the coating microstructure is explained with reference to the appropriate Ni-Al-Nb ternary isotherms and the structural aspects are discussed with the aid of diffusion kinetics. Although only one coating-substrate system was used, the conclusions drawn from the present study are expected to be common to most, if not all, aluminide-coated directional eutectics.

#### EXPERIMENTAL PROCEDURES

Specimens for aluminization were sectioned from a directionally solidified  $\gamma'/\delta$  alloy (nominal composition 15.1<sup>a</sup>/o Nb-75<sup>a</sup>/o Ni-9.9 Al), so that the growth direction was parallel to the plane of the section. After grinding on 600 grit SiC paper, the specimens were degreased and aluminized using the pack-cementation process.<sup>7,8,10</sup> The details of the aluminizing treatment are given in Table I. Temperatures of 900°C and 1140°C were chosen because of the availability of ternary isotherms.<sup>13,14</sup>

Homogenizing treatments were done in an argon atmosphere at 900°C and 1140°C for times ranging from 1 to 150 hr. These times provided sufficient coating degradation to permit the formulation of degradation mechanisms.

A combination of metallography, electron microprobe analyses (EMPA) and X-ray diffraction techniques (for the surface phases) were

used for phase identification. Microprobe intensities from three line emissions (Nb  $L\alpha$ , Ni  $K\alpha$ , Al  $K\alpha$ ) were recorded by point and line counting at successive steps parallel to the diffusion direction; raw intensities were corrected for background and dead-times and converted to concentration values using the alpha-coefficient method.<sup>15</sup> Diffusion paths along each of the original  $\gamma'$  and  $\delta$  lamellae were determined by plotting concentration values on the ternary isotherms.

## RESULTS

### A. Aluminization of the Substrates

Figs. 1(a) and (b) show the as-aluminized microstructure of a directional  $\gamma'/\delta$  eutectic at 900°C and 1140°C, respectively, formed by pure aluminum in the coating pack (high-aluminum activity pack). Basically, both the microstructures showed evidence of the original lamellar morphology, as seen in zone A, Figs. 1(a) and (b). However, the phases present in that zone differed at the two temperatures. At 900°C,  $Ni_2Al_3$  and  $NbAl_3$  were present whereas at 1140°C, a layer of Al-rich  $\beta$  and  $NbAl_3$  was formed above a layer of Al-rich  $\beta$  and Nb  $(Ni_xAl_{1-x})_2$  ( $\lambda$ ). In addition, at 1140°C, Fig. 1(b), another region (zone B) was prominent. It consisted of a layer of  $Ni_2NbAl$  ( $\eta$ ) at the positions marked by arrows and extensions into the  $\gamma'$  lamellae. EMPA data show the latter to consist of two-phase regions of Ni-rich  $\beta$  and  $\delta$ . (At 900°C, zone B was barely resolved; no conclusions could be reached regarding its composition.)

Fig. 1(c) shows the microstructure of an as-aluminized substrate at 1140°C formed by an alloy of aluminum and nickel in the coating pack

(low-aluminum activity pack, see Table I for pack composition). As in the case of high-aluminum activity packs, the coating microstructure can be divided into zones A and B. Zone B is very similar to that in Figure 1(b) and consists of the  $\eta$ -phase (denoted by arrows) and coating extensions of Ni-rich  $\beta$  and  $\delta$  into the  $\gamma'$  lamellae. Zone A, on the other hand, differs from that in Figs. 1(a) and (b) by the absence of the original lamellar morphology. Particles of aluminum oxide trapped in this zone serve as diffusion markers and indicate the relative motion of the aluminum and nickel atoms.

Figure 2 shows the diffusion paths plotted on the appropriate ternary isotherms for each of the microstructures in Figure 1.

#### B. Homogenization of the Coated Substrates

Figure 3 shows the homogenization sequence for the aluminized substrate  $\sigma$  of Fig. 1(b). The first significant change to occur is the formation of an integral layer of the  $\eta$ -phase in zone B, Fig. 3(a). At a later time, a layer of Ni-rich  $\beta$ , containing no secondary phases, forms above the  $\eta$ -phase, Fig. 3(b). At the end of 50 hrs. of homogenizing, Fig. 3(c), the Al-rich phases of the surface have disappeared, exposing the Ni-rich  $\beta$  layer of composition 3.3<sup>a</sup>/o Nb-59.7<sup>a</sup>/o Ni-37<sup>a</sup>/o Al.

The sequence of homogenization of high-activity packs at 900°C is similar to that at 1140°C, but has slower kinetics. The coating layers after 150 hrs. at 900°C are sequentially similar to those in the as-aluminized microstructure at 1140°C. This is at variance with what was expected since the 900°C isotherm shows the existence of a two-phase region of  $\gamma'$  and  $\eta$ , instead of Ni-rich  $\beta$  and  $\delta$  that appears on the coated substrates. The existence of the  $\gamma'+\eta$  region on the 900°C isotherm is therefore inconsistent with results of the present study.

Figure 4 shows the stages of homogenization of a substrate aluminized with a low-aluminum activity pack at  $1140^{\circ}\text{C}$ . The first stage involves the disappearance of the  $\eta$ -phase, Fig. 4(a) and the consequent joining of the Ni-rich  $\beta$  in zones A and B, Fig. 4(b). At the end of 150 hrs., zone A is separated from the  $\gamma'/\delta$  substrate by a layer of  $\gamma'$ .

### DISCUSSION

#### A. The Mechanism of Coating Formation

The preceding section has indicated several similarities and differences between the microstructures in Fig. 1. Zone A in Figs. 1(a) and (b) possesses the original lamellar morphology whereas this is not evident in Fig. 1(c). Zone B is very similar in Figs. 1(b) and (c) whereas it is not resolved in Fig. 1(a). A spectrum of coating microstructures can, therefore, be obtained by altering the aluminizing process variables, limited at one end by low aluminizing temperatures and high aluminum activity packs and at the other by high aluminizing temperatures and low-aluminum activity packs.

In general, the surface phases present on the coatings are determined by the constitution of the Ni-Al-Nb ternary isotherm, or more precisely, by the aluminizing temperature and the activity of aluminum in the coating pack. In high-activity packs, the phases with the highest aluminum content form along the original  $\gamma'$  and the  $\delta$  lamellae. These are  $\text{Ni}_2\text{Al}_3$  at  $900^{\circ}\text{C}$  and Al-rich  $\beta$  at  $1140^{\circ}\text{C}$  (above the melting point of  $\text{Ni}_2\text{Al}_3$ ) along the  $\gamma'$  lamellae and  $\text{NbAl}_3$  at both temperatures along the  $\delta$  lamellae. However, the ternary isotherm indicates that both  $\text{Ni}_2\text{Al}_3$  and

Al-rich  $\beta$  have lower solubilities of niobium than the original  $\gamma'$ -phase. Thus Nb-enriched secondary phases must precipitate. These phases precipitate along the original  $\delta$  lamellae since  $\text{NbAl}_3$  is almost stoichiometric. Consequently, in high-activity packs, the surface layers consist of two-phase regions along each of the original  $\gamma'$  and  $\delta$  lamellae. This is observed in the diffusion paths in Fig. 2.

The diffusion paths originating from the surface phases alternately have to reach the composition of the substrate ( $\gamma'$  and  $\delta$ ). In doing so they have to cross various single-phase, two-phase and three-phase fields. At  $1140^\circ\text{C}$ , these are Al-rich  $\beta + \lambda$ ,  $\beta + \eta$ , Ni-rich  $\beta + \delta$  and  $\gamma'$ , along the  $\gamma'$  lamellae and Al-rich  $\beta + \lambda$ ,  $\eta$  and  $\delta$  along the  $\delta$  lamellae. At  $900^\circ\text{C}$ , the identity of the two-phase fields could not be determined.

The sequence of phase layers in low-aluminum activity coatings can also be explained with reference to the ternary phase diagram. The surface phase of stoichiometric  $\beta$  forms because it corresponds to the activity of aluminum being transported to the surface of the substrate. However, due to the low solubility of niobium in the  $\beta$ -phase, a Nb-enriched secondary phase precipitates. The diffusion path in Fig. 2(a) traverses the two-phase Ni-rich  $\beta + \delta$  region and terminates in the  $\gamma'$ -phase, along the  $\gamma'$  lamellae and passes through the  $\eta$  and  $\delta$ -phases, along the  $\delta$  lamellae.

The structural aspects of the coating layers can now be discussed with the aid of appropriate diffusion data. Clearly, the manner in which zone A formed in Figs. 1(a) and (b) is different from the manner in which it formed in Fig. 1(c). Also, the structural similarity at zone B in Figs. 1(b) and (c) suggests that it formed differently than in Fig. 1(a).

These similarities and differences can be explained from the relative rates of motion of the mobile species during coating formation.

Although no diffusion data exist for the Ni-Al-Nb ternary system, data are available for the respective binary systems. Such data aid in making assumptions as to which species is the most mobile. Table II lists the appropriate binary systems and the most mobile species in the phases of interest. Zone A in Figs. 1(a) and (b) contains  $Ni_2Al_3$ , Al-rich  $\beta$  and  $NbAl_3$  and hence must form by the predominant diffusion of aluminum atoms along the original  $\gamma'$  and the  $\delta$  lamellae. The lamellar morphology of the zone is consequently retained. In Fig. 1(c), zone A consists of stoichiometric  $\beta$  and in this phase nickel atoms are more mobile than aluminum atoms (Table II). The nickel atoms move outward and react with aluminum on the external surface. In doing so, the layer of stoichiometric  $\beta$  which forms loses the original lamellar morphology of the substrate. The outward motion of nickel is evidenced by the entrapment of aluminum oxide particles within the outer coating layers.

Zone B in Figs. 1(b) and (c) consist of Ni-rich  $\beta$  and  $\delta$ . In these phases nickel is the mobile species (Table II). Nickel atoms move out of the  $\gamma'$ -phase, making it rich in aluminum and niobium and resulting in the formation of Ni-rich  $\beta$  and  $\delta$ . This zone is not evident at  $900^\circ C$ , Fig. 1(a), due to the combination of the high inter-diffusion coefficient of the  $Ni_2Al_3$  phase and the low aluminizing temperature, which retards the formation of Ni-rich phases.

In general, the diffusion rate of nickel out of the original  $\gamma'$  and the  $\delta$  lamellae will not necessarily be the same;<sup>21</sup> lateral diffusion

across the original  $\gamma'/\delta$  interphase boundary might be expected. This effect is observed during the formation of the  $\eta$ -phase layer in Figs. 1(b) and (c). At the positions denoted by arrows, the  $\delta$ -lamellae would be juxtaposed with a layer of  $\beta$  containing about 5<sup>a</sup>/o Nb-54<sup>a</sup>/o Ni-41<sup>a</sup>/o Al. However, such a situation cannot occur due to the phase equilibria on the 1140<sup>o</sup>C isotherm and so an intervening layer of the  $\eta$ -phase must form. This occurs by the transverse dissolution of the  $\beta$ -phase.

#### B. The Mechanism of Coating Degradation in an Inert Environment

Once the coating layers have been formed with Al-rich phases on the surface of the substrate, the inward diffusion of aluminum continues until its concentration gradient cannot support significant inward aluminum diffusion. At this stage a reversal of interface motion occurs<sup>22</sup> and the growth of Ni-rich phases is gradually promoted. This involves a change in the mode of diffusion, from predominant aluminum motion to predominant nickel motion. Figure 3(b) shows a layer of Ni-rich  $\beta$  (in zone A) formed by the simultaneous diffusion of aluminum inward through the Al-rich phases at the surface, nickel diffusion outward from the substrate and the reaction of this nickel with aluminum. The fact that this Ni-rich  $\beta$  layer does not possess the original lamellar morphology and secondary phases, indicates that it was formed by the above mechanism. Eventually, the inward motion of aluminum atoms ceases due to the removal of the Al-rich phases at the surface by the outward growth of the Ni-rich  $\beta$ , Fig. 3(c), and only the motion of nickel atoms through the Ni-rich phases occurs.

In low-aluminum activity pack coatings, since Al-rich surface phases are not present, inward diffusion of aluminum does not occur;

homogenization continues only by the diffusion of nickel atoms from the substrate into the coating layers.

#### SUMMARY

The present study shows that a spectrum of microstructures can be obtained in aluminide coatings on  $\gamma'/\delta$  directional eutectics by proper selection of process variables. A complete description of the coating microstructures requires reference to the appropriate ternary isotherm as well as kinetic data (relative mobility of the aluminum and the nickel atoms). Process variables that form Al-rich phases on the surface promote the inward diffusion of aluminum whereas those which form Ni-rich phases on the surface promote the outward diffusion of nickel atoms from the substrate. The presence of two aligned phases of different composition in the eutectic substrate allows for diffusion across the interphase boundaries, since the diffusion rates along the  $\gamma'$  and the  $\delta$  lamellae are not the same. The above conclusions are expected to be similar for most aluminide-coated directional eutectics.

#### ACKNOWLEDGEMENTS

The authors greatly appreciate the financial support of the Metallurgy Branch of the Office of Naval Research. They also wish to thank Dr. G. W. Goward, Pratt & Whitney Aircraft for his interest and supply of the substrate material, and Dr. L. F. Vassamillet, Carnegie-Mellon University for his assistance in electron microprobe analysis.

REFERENCES

- 1 E. R. Thompson and F. D. Lemkey, *Am. Soc. Met., Trans. Q.*, 62 (1969) 140.
- 2 E. J. Felten and F. S. Pettit, in J. N. Fleck and R. L. Mehan (Eds.), *Failure Modes in Composites II*, Am. Inst. Min., Metall. Eng., Inst. Met. Div., New York, 1974, p. 220
- 3 J. G. Smeggil and M. D. McConnell, *Oxid. Met.*, 8 (1974) 309.
- 4 E. J. Felten, T. E. Strangman and N. E. Ulion, *Coatings for Directional Eutectics*, NASA Cr-134735, Pratt & Whitney Aircraft, East Hartford, Conn., 1974.
- 5 G. W. Goward and D. H. Boone, *Oxid. Met.*, 3 (1971) 475.
- 6 G. W. Goward, D. H. Boone and C. S. Giggins, *Am. Soc. Met., Trans. Q.*, 60 (1967) 228.
- 7 T. K. Redden, *Trans. Am. Inst. Min., Metall., Pet. Eng.*, 242 (1968) 1695.
- 8 *High-Temperature Oxidation Resistant Coatings*, ISBN 0-309-01769-6, NAC, NMAB, 1970.
- 9 S. J. Grisaffe, in C. T. Sims and W. C. Hagel (eds.), *The Superalloys*, John Wiley and Sons, New York, 1972, p. 341.
- 10 S. R. Levine and R. M. Caves, *J. Electrochem. Soc.*, 121 (1974) 1051.
- 11 J. B. Clark and F. N. Rhines, *Am. Soc. Met., Trans. Q.*, 51 (1959) 199.
- 12 J. S. Kirkaldy and L. C. Brown, *Can. Metall. Q.*, 2 (1963) 89.
- 13 J. S. Benjamin, B. C. Giessen and N. J. Grant, *Trans. Am. Inst. Min. Metall., Pet. Eng.*, 236 (1966) 224.
- 14 V. Ya Markiv, M. F. Matushevskaya and Yu. B. Kuz'ma, *Russ. Metall.*, 6 (1966) 72.
- 15 D. Laguitton, R. Rousseau, and F. Claise, *Anal. Chem.*, 47 (1975) 2174.
- 16 M. M. P. Janssen and G. D. Rieck, *Trans. Am. Inst. Min., Metall. Pet. Eng.*, 239 (1967) 1372.
- 17 M. M. P. Janssen, *Metall. Trans.*, 4 (1973) 1623.
- 18 A. J. Bradley and A. Taylor, *Phil. Mag.*, 23 (1937) 1049.
- 19 G. Slama and A. Vignes, *J. Less-Common Met.*, 29 (1972) 189.
- 20 Y. Muramatsu, *Trans. Nat. Res. Inst. Met.*, 17 (1975) 21.
- 21 S. Z. Bokshteyn, M. A. Gubareva, S. T. Kishkin and L. M. Moroz, *Phys. Met. Metallogr.*, 37 (1974) 104.

TABLE I

Aluminizing Times, Temperatures and the Composition for High and Low-Aluminum Activity Packs.

Type of Coating	Aluminizing Temperature (°C)	Aluminizing Time (hr)	Pack Composition (w/o)		
			Inert filler (Al <sub>2</sub> O <sub>3</sub> )	Activator NH <sub>4</sub> Cl	Pure Aluminum
High-Aluminum Activity Pack	900	0.33	72.0	3.0	25.0
	1140	0.5	94.0	3.0	3.0
Low-Aluminum Activity Pack	1140	1.0	72.0	3.0	25.0

Aluminum Alloy  
(45<sup>a</sup>/o Ni-55<sup>a</sup>/o Al)

TABLE II  
 The Mobile Species in the Ni-Al, Al-Nb, Ni-Nb and Ni-Al-Nb Systems

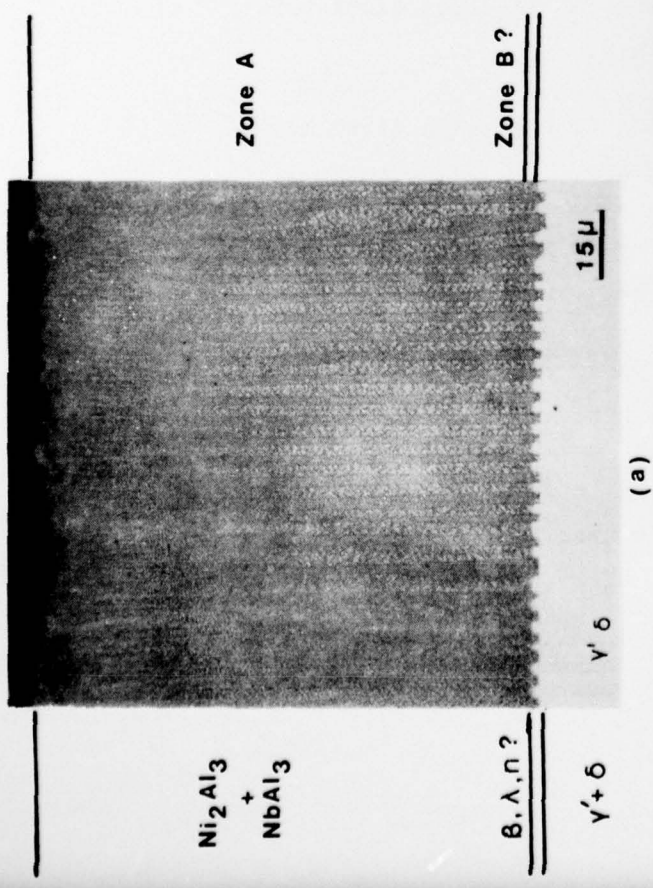
System	Mobile Species in the Following Phases							References
	$NiAl_3(\epsilon)$	$Ni_2Al_3$	Al-rich $\beta$	Ni-rich $\beta$	$\gamma'$	$\gamma$	$\delta$	
Ni-Al	Al	Al	Al	Ni	Ni	Al	-	16, 17, 18, 5
Al-Nb	-	-	-	-	-	-	-	19
Ni-Nb	-	-	-	-	-	-	Ni	20
Ni-Al-Nb	<sup>63</sup> Ni diffuses faster in $\gamma'$ than in $\delta$							21

Stoichiometric  
and

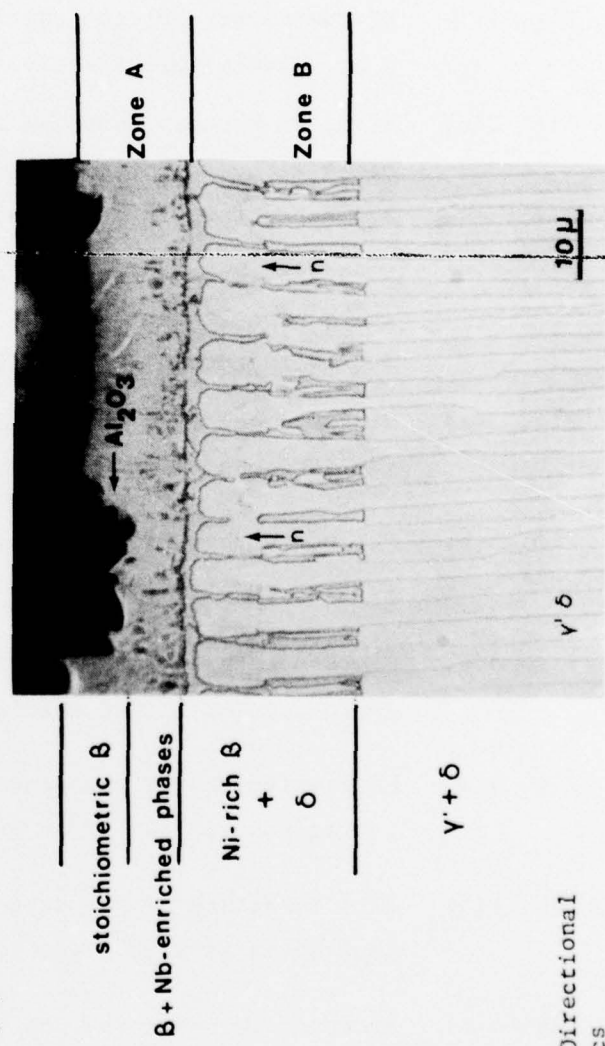
$NbAl_3$

LIST OF FIGURES

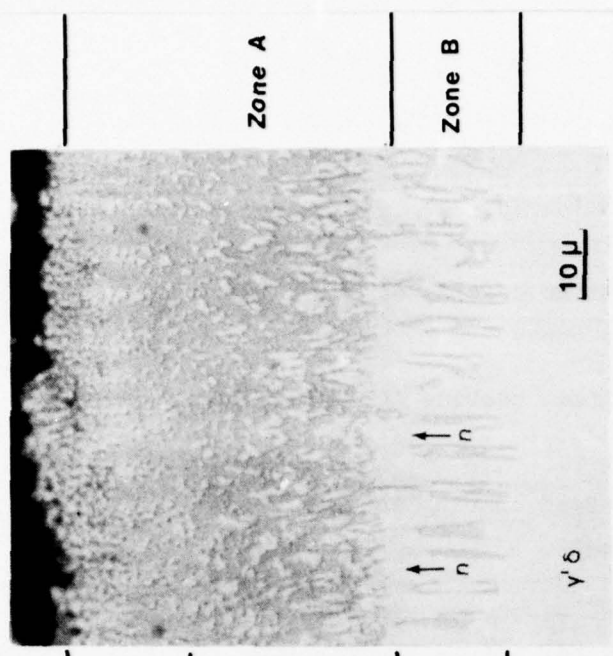
- Fig. 1 (a) Microstructure of the as-aluminized coating at  $900^{\circ}\text{C}$  for 20 min. (high-aluminum activity pack).
- Fig. 1(b) Microstructure of the as-aluminized coating at  $1140^{\circ}\text{C}$  for 30 min. (high-aluminum activity pack).
- Fig. 1(c) Microstructure of the as-aluminized coating at  $1140^{\circ}\text{C}$  for 1 hr. (low-aluminum activity pack).
- Fig. 2(a) Ni-Al-Nb ternary isotherm at  $900^{\circ}\text{C}$  showing the diffusion paths along the original  $\gamma'$  and the  $\delta$  lamellae for the microstructure in Fig. 1(a).
- Fig. 2(b) Ni-Al-Nb ternary isotherm at  $1140^{\circ}\text{C}$  showing the diffusion paths along the original  $\gamma'$  and the  $\delta$ -lamellae for the microstructures in Fig. 1(b) and (c).
- Fig. 3(a) Microstructure of the coating in Fig. 1(b) after homogenization at  $1140^{\circ}\text{C}$  for 1 hr.
- Fig. 3(b) Microstructure of the coating in Fig. 1(b) after homogenization at  $1140^{\circ}\text{C}$  for 3 hrs.
- Fig. 3(c) Microstructure of the coating in Fig. 1(b) after homogenization at  $1140^{\circ}\text{C}$  for 50 hrs.
- Fig. 4(a) Microstructure of the coating in Fig. 1(c) after homogenization at  $1140^{\circ}\text{C}$  for 1 hr.
- Fig. 4(b) Microstructure of the coating in Fig. 1(c) after homogenization at  $1140^{\circ}\text{C}$  for 50 hrs.
- Fig. 4(c) Microstructure of the coating in Fig. 1(c) after homogenization at  $1140^{\circ}\text{C}$  for 150 hrs.



(a)



(c)



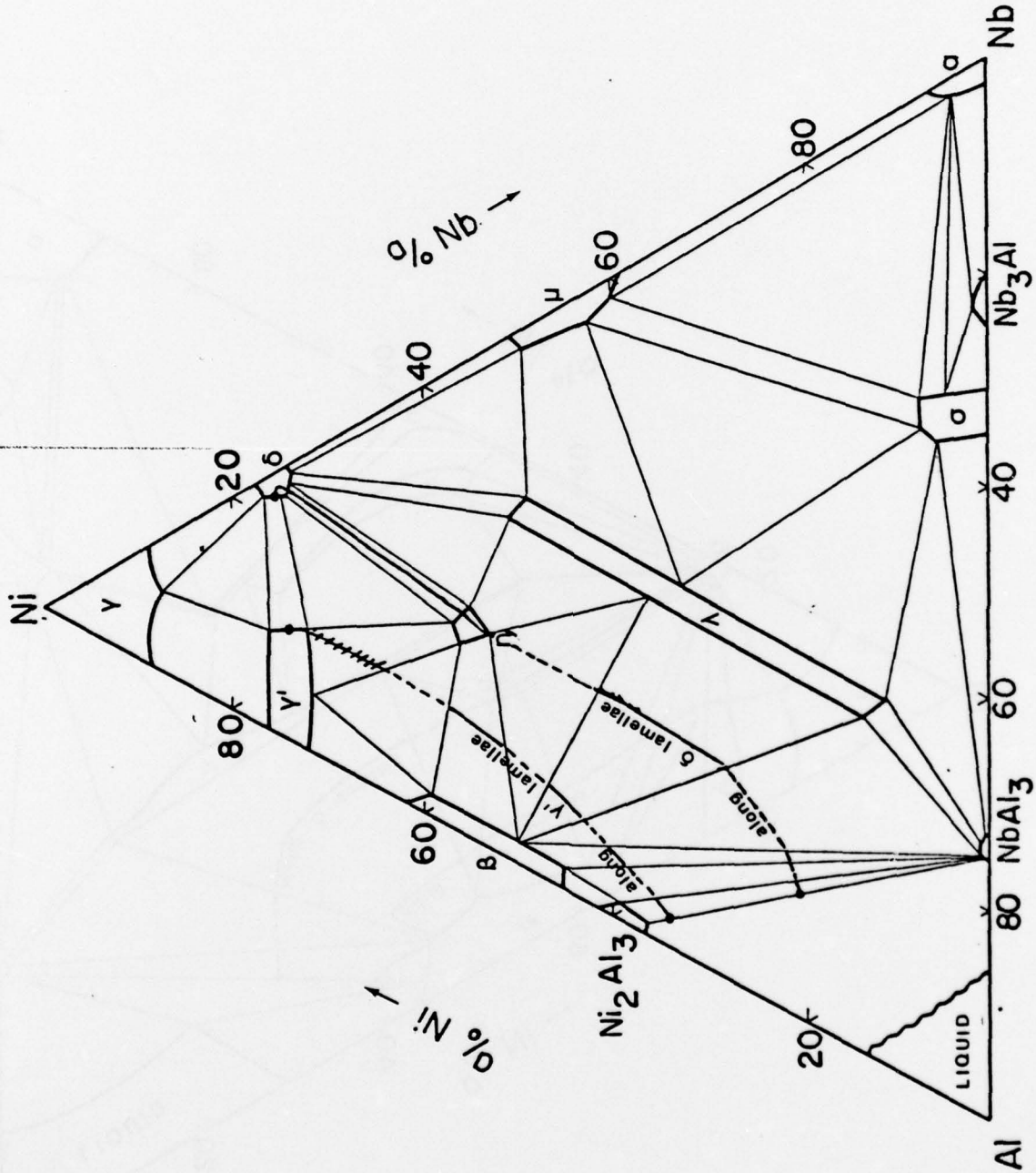
(b)

Aluminide Coating on Directional  $\gamma/\delta$  Eutectics

H.C. Bhedwar, R.W. Heckel & D.E. Laughlin

FIGURE 1

DIFFUSION PATHS ON THE 900°C ISOTHERM



← % Al

FIGURE 2(a)

Aluminide Coating on Directional  $\gamma'/\delta$  Eutectics

H.C. Bhedwar, R.W. Heckel & D.E. Laughlin

DIFFUSION PATHS ON THE 1140°C ISOTHERM

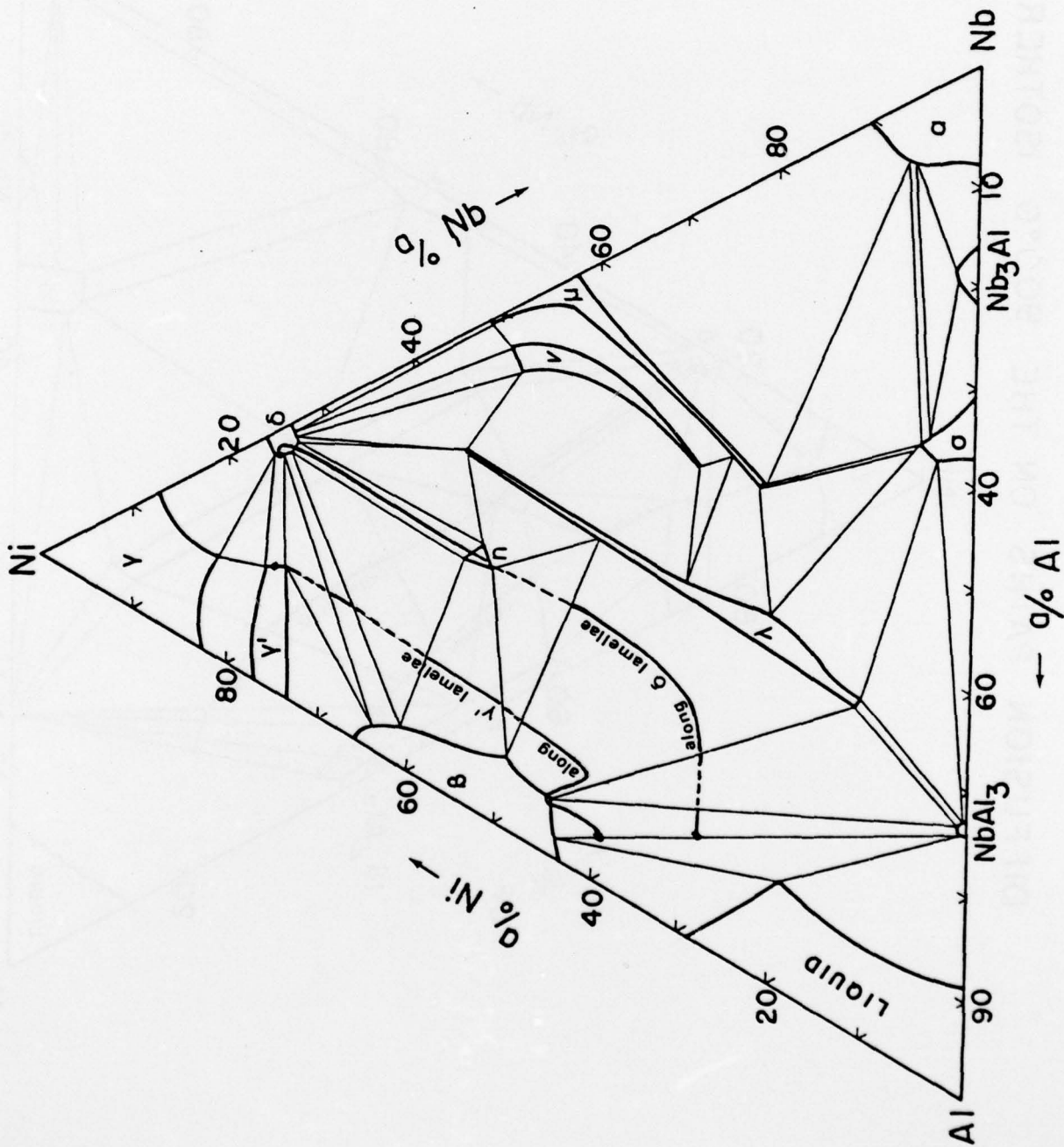
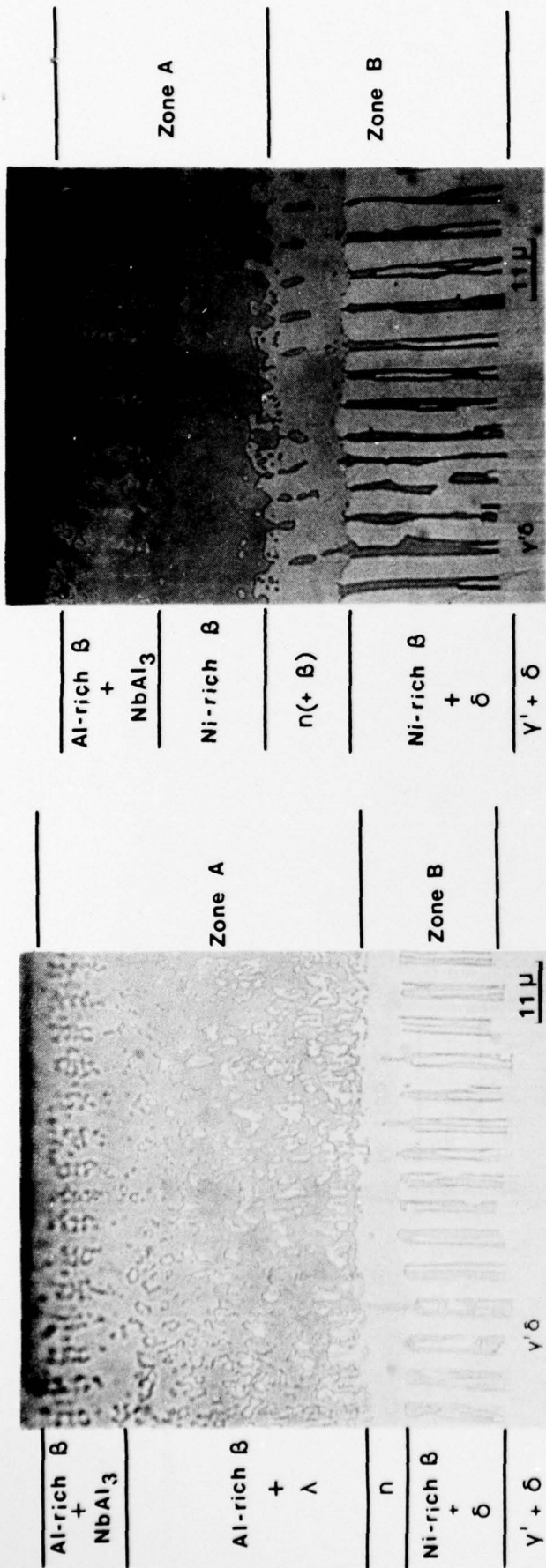
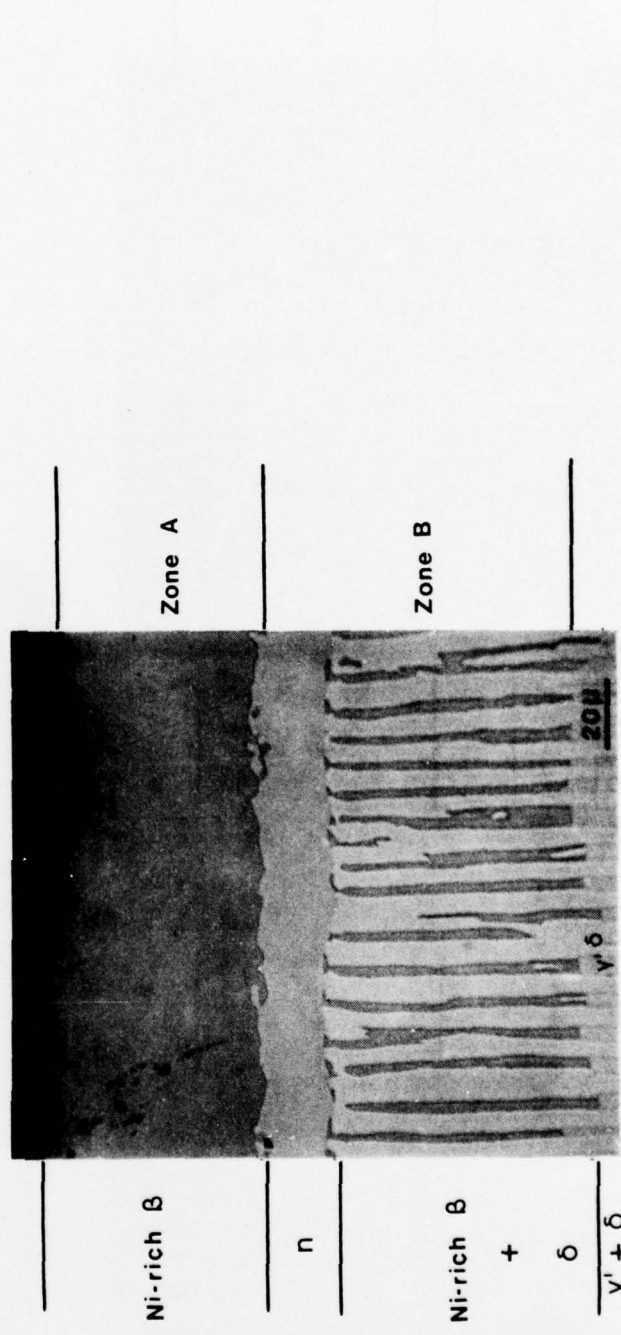


FIGURE 2 (b)

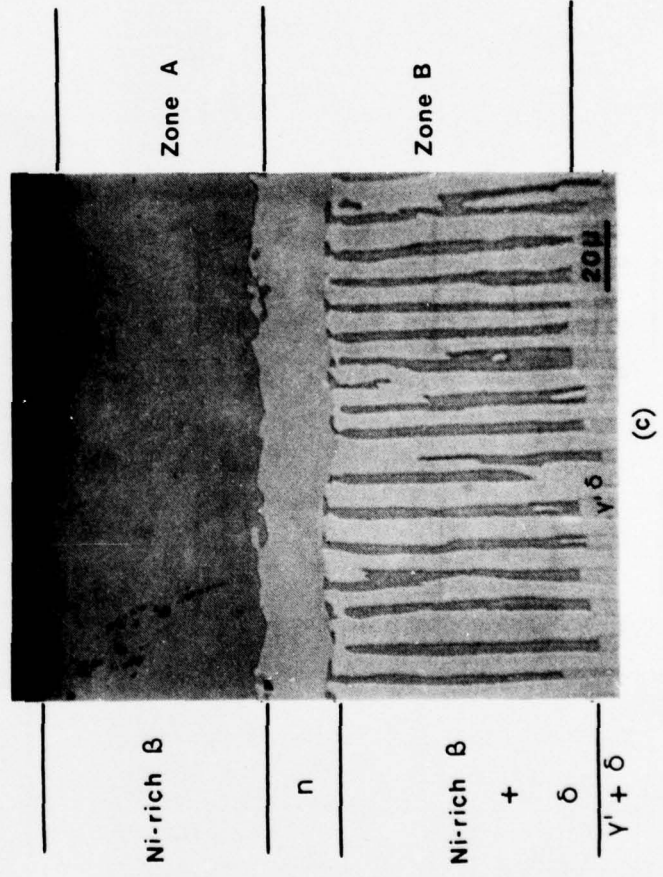
Aluminide Coating on Directional  $\gamma'/\delta$  Eutectics  
 H.C. Bhedwar, R.W. Heckel & D.E. Laughlin



(a)

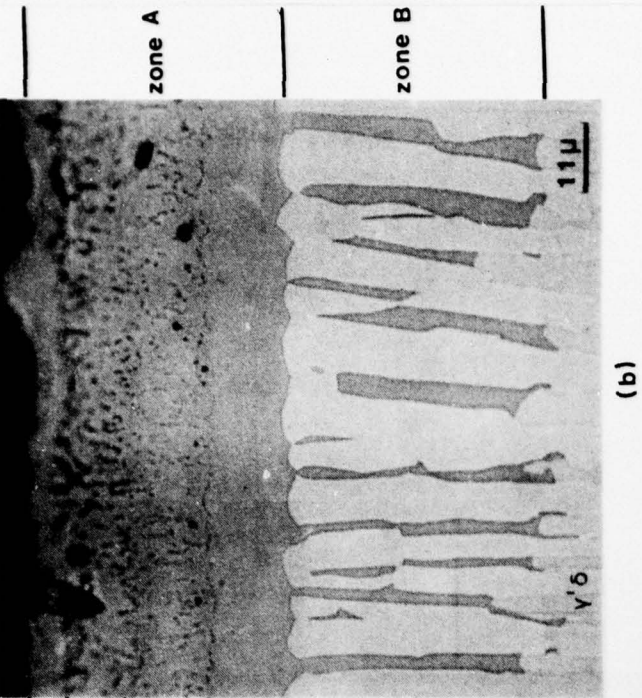


(b)



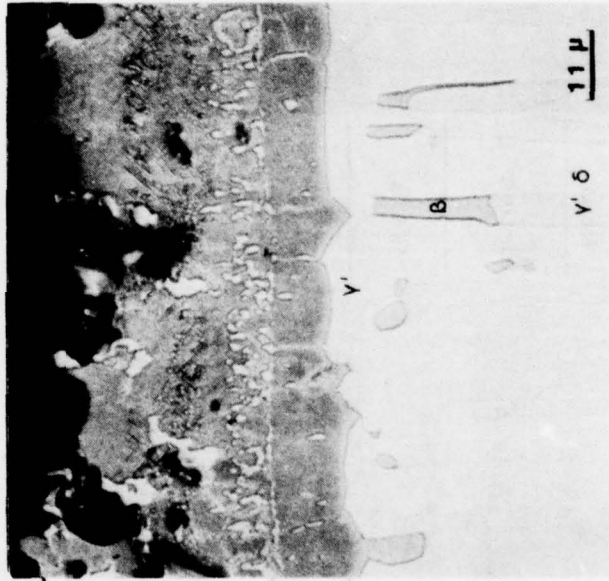
(c)

Aluminide Coating on Directional  $\gamma' / \delta$  Eutectics  
 H.C. Bhedwar, R.W. Heckel & D.E. Laughlin



stoichiometric  $\beta$   
 Ni-rich  $\beta + \lambda$   
 Ni-rich  $\beta + n$   
 Ni-rich  $\beta$   
 n  
 Ni-rich  $\beta$   
 +  
 $\delta$   
 $\gamma' + \delta$

(a)



Ni-rich  $\beta$   
 Ni-rich  $\beta + \lambda$   
 Ni-rich  $\beta + n$   
 Ni-rich  $\beta$

(b)

Aluminide Coating on Directional  $\gamma' / \delta$  Eutectics

H.C. Bhedwar, R.W. Heckel & D.E. Laughlin

FIGURE 4

